Electron spin resonance and microwave magnetoresistance in Ge:Mn thin films

R. Morgunov,[1] M. Farle,[2] M. Passacantando,[3] L. Ottaviano,[3] and O. Kazakova[4,*]
[1]*Institute of Problems of Chemical Physics, Chernogolovka 142432, Russia*
[2]*Fachbereich Physik and Center for Nanointegration (CeNIDE), Universitat Duisburg-Essen, Duisburg 47048, Germany*
[3]*CNR and Dipartimento di Fisica, Università dell'Aquila, Coppito L'Aquila 67010, Italy*
[4]*National Physical Laboratory, Teddington TW11 0LW, United Kingdom*
(Received 11 December 2007; revised manuscript received 12 May 2008; published 14 July 2008)

We report a study of resonant and nonresonant microwave absorption in germanium thin films (t=120 nm) implanted with manganese to a concentration of x=2–8 at. %. The germanium matrix contains Mn_5Ge_3 precipitates, Mn-rich ferromagnetic nanoclusters, and diluted Mn ions. Electron spin resonances (ESR) observed below 60 K are attributed to collective spin waves in the whole film, while at higher temperatures resonances due to ferromagnetic Mn_5Ge_3 precipitates are detected. The high-frequency magnetoresistance (MR) exhibits a nonmonotonic field behavior with a minimum around H=1–4 kOe. The orientation dependence of the MR is explained by dimensional effects in the thin film geometry and inhomogeneous distribution of magnetic centers. A phase relaxation length of band carriers in Ge:Mn films is determined. It varies from 70–350 nm with decreasing temperature and exceeds the mean intercluster distance in the whole temperature range. This implies that the intrinsic conductivity of the nanoclusters does not generally influence the MR, and the main contribution to the microwave MR originates from charge carriers.

DOI: 10.1103/PhysRevB.78.045206 PACS number(s): 75.50.Pp, 75.70.−i, 76.30.Fc, 76.50.+g

I. INTRODUCTION

Both semiconductors and magnetic materials play an important role in modern electronics. Conventional electronic devices utilize the electron (hole) charge to process and store information. The use of an electron spin holds great promise for a new class of semiconductor memory and signal processing devices with a new functionality. Coexistence of magnetism and semiconducting properties has been realized in diluted magnetic semiconductors (DMS) (Refs. 1 and 2) and metal-organic salts doped with transition ions. Generally, these types of materials have low Curie temperatures, which make them unsuitable for industrial applications. However, unusual magnetic properties of nanostructures based on Ge or Si hosts doped with Mn have been demonstrated recently.[3–9] High Curie temperature, correlation between electrical and magnetic properties,[10–12] existence of weakly-localized charge and spin carriers in a magnetically ordered lattice, and other remarkable features of these systems make them particularly attractive for spintronic applications. Detailed investigations and comparison of bulk,[13] two-dimensional (2D) Ge:Mn magnetic films (see, for example, Refs. 14–22) and quasi-one-dimensional $Ge_{1-x}Mn_x$ nanostructures[3–6,8] have been performed recently. Generally, in thin films a nonmonotonic dependence of the magnetoresistance (MR) on magnetic field and temperature was observed and attributed to a complex film structure containing various types of magnetic clusters. These findings were discussed in terms of a combination of the hopping electrical conductivity, Zeeman splitting, spin-dependent scattering on bounced magnetic polarons, and geometrical MR of nanoclusters. It was also shown that the MR ratio may vary from ~1% (Refs. 19, 21, and 22) to 270% (Ref. 20) depending on the film composition, growth method, and sample history. None of these works, however, provides any direct evidence of the MR effect observed in $Ge_{1-x}Mn_x$ or $Si_{1-x}Mn_x$ nanowires. In all works cited above the MR was measured using conventional contacting techniques. On the other hand, a contact free method based on measurements of the resistivity change in a microwave cavity and simultaneous detection of electron spin resonance (ESR) has been successfully used both for thin films[23–25] and nanoscale objects.[26] For samples with low resistivity, ρ, the absorbed microwave power P changes as a function of magnetic field H;

$$P \propto \rho(H) \quad \text{and} \quad dP/dH \propto d\rho(H)/dH, \tag{1}$$

as, for example, was demonstrated in semiconductors.[27,28]

In this work we study both the resonant and nonresonant microwave absorption at 9.45 and 24.17 GHz in Mn-implanted Ge thin films as a function of temperature and Mn concentration. In particular, we provide evidence for the existence of long-range ($k \geq 0$) spin waves at low temperatures and attribute high-temperature ESR resonances to spatially separated noninteracting Mn_5Ge_3 nanoclusters. Possible mechanisms of the observed nonresonant absorption of magnetoresistive origin are discussed. We demonstrate that the intrinsic conductivity of the nanoclusters does not generally influence the MR and that the main contribution to the microwave MR originates from charge carriers.

II. EXPERIMENT

Ge:Mn thin films were prepared by implanting Mn^+ ions into commercially purchased single-crystal Ge(100) wafers (resistivity=40–57 Ohm cm). Mn^+ ions were implanted with an energy of 100 keV at fluences of 1×10^{16}, 2×10^{16}, and 4×10^{16} at./cm^2. These fluences produce average volume concentrations of Mn of about 2, 4, and 8 at.%, respectively, on top of the Ge substrate. During the implantation, the samples were held at 300 °C to avoid amorphization. The projected depth range of Mn ions is about 120 nm with the implant designed to yield a quasi-Gaussian profile.[29]

Structural, electronic, and static magnetic properties of the samples have been extensively studied earlier by a number of experimental techniques.[29–32] We want to emphasize a thorough control of the sample fabrication. Indeed, preparation of samples under the same conditions (density and energy of the ion flux, substrate temperature, etc.) always results in an identical type of samples, i.e., characterized by the same Mn profile, type of Mn defects, ratio of diluted and precipitated Mn, etc. Three samples with different Mn concentration considered in the paper represent three different types of magnetic semiconductors, which could be obtained by ion implantation:

(1) $x=2\%$—low Mn concentration, small amount of amorphous semiconducting Mn-rich nanoclusters with a mean diameter below 7.5 nm, complete absence of ferromagnetic Mn_5Ge_3 precipitates.

(2) $x=4\%$—an optimal ratio between diluted Mn and phase precipitation; metallic Mn_5Ge_3 crystalline clusters with a mean diameter of 9.5 nm.

(3) $x=8\%$—large amount of Mn_5Ge_3 precipitates at the expense of the Mn diluted phase; metallic Mn_5Ge_3 crystalline clusters with a mean diameter of 13.1 nm.

Magnetization measurements were performed using a superconducting quantum interference device (SQUID) magnetometer (MPMX 5XL, Quantum Design) at temperatures between 1.8 and 370 K and in fields up to 50 kOe. A magnetic field was applied either in the plane or perpendicular to the plane of the sample.

The ESR experiments have been performed in a conventional ESR spectrometer (EMX Bruker) equipped with an ESR-910 cryostat (Oxford Instrument). Technical details of the experimental setup have been given elsewhere.[23] Angular dependent (both in plane and out of plane) magnetic resonance spectra were measured as a function of magnetic field at microwave frequencies of 9.45 and 24.17 GHz and a modulation frequency of 100 kHz between 4 and 310 K. It should be noted that the majority of measurements have been performed at 9.45 GHz, unless specified differently. The following methodology was adapted to provide an interpretation of the angular dependencies: when the field is applied in the plane of an isotropic film, the resonance occurs at the frequency ω_0 of the spin-wave mode with the wave number $q=0$ propagating along the film:[33]

$$\omega_0 = \gamma[H(H+4\pi M+H_s)]^{1/2} - \delta\omega_0, \tag{2}$$

where $\gamma=g\mu_B/\hbar$ is the gyromagnetic ratio, M is the saturation magnetization, $H_s=2K_s/Mt$ is the surface anisotropy field, t is the film thickness, and $\delta\omega_0$ is the frequency shift due to the spin-wave energy renormalization processes. In a two-dimensional system the angular dependence of the resonant field H_{res} can be described by following equations:[33]

$$\omega/\gamma = \sqrt{H_1 H_2},$$

$$H_1 = H_{\mathrm{res}}\cos(\theta_H-\theta) - 4\pi M_{\mathrm{eff}}\cos 2\theta,$$

$$H_2 = H_{\mathrm{res}}\cos(\theta_H-\theta) - 4\pi M_{\mathrm{eff}}\cos^2\theta, \tag{3}$$

where θ_H is the angle between the film plane and the external dc magnetic field and θ is the angle between the film magnetization vector M and the film plane.

Samples were placed into a rectangular resonator at an antinode of the microwave magnetic field. In a separate series of experiments performed in a cylindrical resonator at room temperature, we checked that both the displacement of the sample from the resonator axis into regions of a stronger microwave electric field and the dispersion signal did not distort the magnetic resonance spectrum. Variation of the microwave power over several orders of magnitude (in the range $10^{-6}-10^{-2}$ W) also did not change the shape of the spectra. For all geometries the static magnetic field was kept perpendicular to the microwave one.

To exclude the possibility that magnetoelastic surface modes (Walker modes) may cause electron spin resonances, we studied samples of both rectangular and arbitrary shapes. No dependence of ESR spectra on the sample shape was found, thereby excluding this possibility.

The intensity (hence, static magnetic susceptibility[34]) of the ESR resonances of the Mn:Ge films were calibrated against a paramagnetic single crystalline $CuSO_4\cdot 5H_2O$ 99.99% pure standard for which a total number of spins, $N=2\times 10^{17}$, corresponding to Cu^{2+} ions with $S=1/2$ was determined by SQUID magnetometry ($T=4-300$ K). Line positions were calibrated against a standard paramagnetic α'-diphenyl-β-picryl hydrazyl (DPPH) sample. In order to study the MR effect, the absorptive background of the cavity was measured for all experimental conditions and subtracted from each spectrum. One should note that in semiconductors with a dopant concentration level in the order of 1%–10% the sampling depth, i.e., the skin depth, is of the orders of tens of microns at 9.45 and 24.17 GHz, which exceeds the thickness $t\cong 120$ nm of the magnetically doped semiconductor film by far. An undoped germanium wafer was measured for comparison and its signal subtracted when necessary.

III. RESULTS

A cross-sectional TEM image showing the morphology of the Mn-implanted Ge film ($x=4\%$) is presented in Fig. 1. The figure reveals the presence of three structural layers: (i) a 120-nm-thick magnetically doped layer containing small Mn_5Ge_3 clusters, Mn-rich amorphous clusters, and diluted Mn ions, (ii) a 100-nm-thick damaged Ge underlayer with "extended defects" (mainly vacancies and Ge interstitials), and (iii) an undistorted Ge substrate.

The ESR spectra of Ge:Mn films exhibit strong temperature dependence. Three main temperature intervals can be distinguished: low ($T=4-60$ K), intermediate ($T=60-220$ K), and high ($T=220-300$ K) temperatures as discussed in the following.

A. Low-temperature regime ($T=4-60$ K)

Complex magnetic resonance spectra containing a number of peaks are observed in Ge:Mn films with different Mn

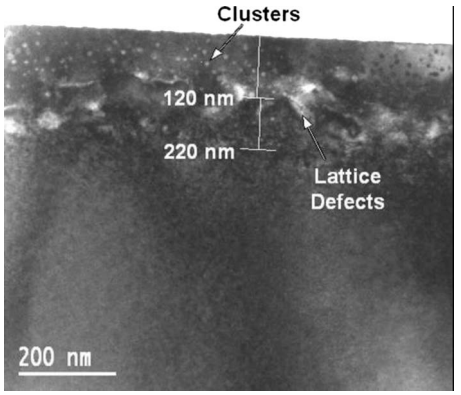

FIG. 1. TEM image showing a cross-section of the ion-implanted Ge:Mn film with Mn concentration of 4%.

concentrations in the temperature range $T=4-60$ K (Fig. 2). For the sample containing 4% of Mn it was possible to clearly identify resonant lines at all temperatures and field orientations. Besides, this sample has optimal structural properties, e.g., the ratio between diluted and precipitated Mn. Its spectrum comprises three strong resonances (labeled 1–3) in the low magnetic-field range ($H<2$ kOe) and two weak lines, which we denote PM1 and PM2, at $H \cong 3.4$ kOe. Investigation of a reference sample (nonimplanted single crystalline Ge wafer, $x=0\%$) shows much simpler ESR spectrum containing lines PM1 and PM2 only. The resonant fields for lines PM1 and PM2, $H=3300-3450$ Oe at 9.45 GHz (i.e., $g=1.975-1.950$), are typical for paramagnetic resonances, which could arise from initial structural defects, a small amount of paramagnetic impurity in the wafer, band carriers in germanium, or a combination of these factors. Henceforth, we shall only consider lines 1–3, which are characteristic of magnetically doped Ge:Mn films. Lines 1–3 exist at $T=4-60$ K only [see Figs. 2 and 3(a)]. The

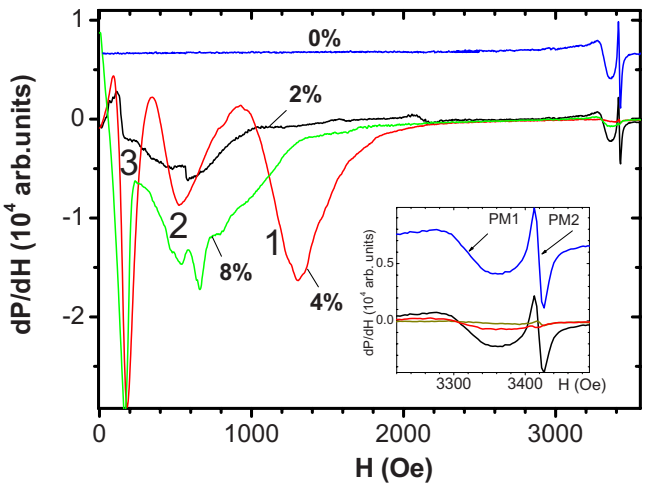

FIG. 2. (Color online) ESR spectra of Ge films implanted with Mn concentration of 0%, 2%, 4%, and 8% at $T=5$ K. Line numbers are given for the sample with the Mn concentration of 4%. The dc magnetic field is oriented at 45 degrees to the film surface. Details of ESR spectra in the $g=2$ region (lines PM1 and PM2) are shown in the inset.

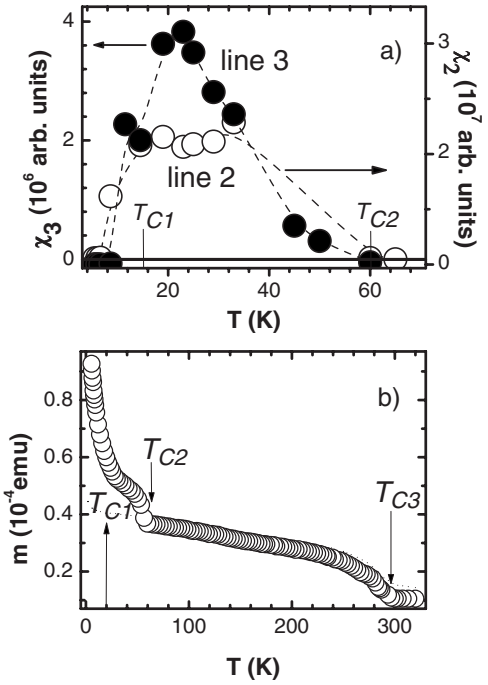

FIG. 3. Temperature dependencies of: (a) magnetic susceptibilities calculated for lines two and three (see Fig. 2) and (b) magnetic moment measured during field cooling in the magnetic field, $H=1$ kOe, in the Ge:Mn film ($x=4\%$). Dashed lines in Fig. 3(a) are guides for the eye. The dc magnetic field is normal to the film plane, $\Theta_H=90$ deg.

temperature dependence of the magnetic susceptibility $\chi_i (i=1-3)$, determined in relative units from the integral intensity of the resonances, is shown in Fig. 3(a) for lines two and three. If to assume that all Mn ions (3×10^{14} ions for $x=4\%$)[29] are (1) in the Mn^+ oxidation state with the largest electronic spin ($3d^5 4s^1$, $S=6/2$) and (2) in the noninteracting paramagnetic state, then calibration against the reference sample demonstrates that the experimental χ_i values exceed the total magnetic susceptibility of such ions by two orders of magnitude. Hence, these resonances cannot be attributed to noninteracting Mn^+ ions and can only be related either to separated superpara- or ferromagnetic centers (for example, ferromagnetic Mn_5Ge_3 clusters and interacting diluted Mn ions) or collective spin excitations in the whole film. Interestingly, SQUID measurements reveal a well-pronounced step at $T_{c2} \approx 60$ K corresponding to the second critical temperature [Fig. 3(b)] at which lines 1–3 disappear. Variation of the Mn concentration leads to similar temperature dependencies of resonant lines. In samples with the Mn concentration of $x=2\%$ and 8% the resonant lines emerged and disappeared in the same temperature range as in the main investigated sample ($x=4\%$). However, the correspondent ESR spectra had a very complex shape, which made a reliable decomposition of the spectrum impossible. Thus, concentration variations of the spectra reflect the structural difference of the investigated Ge:Mn films.

At $T=4$ K the resonance fields H_{res} (lines 1–3) show the same anisotropic response during rotation of the sample around the axis parallel to the film plane, as demonstrated in Fig. 4(a) for line one. This indicates uniform ferromagnetic

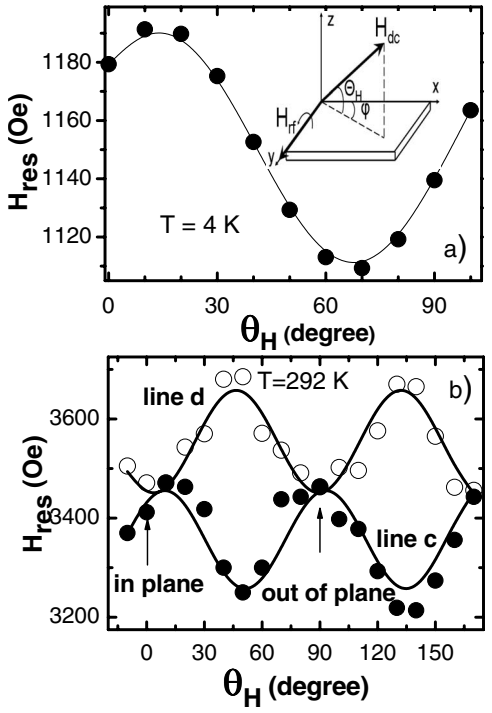

FIG. 4. Angular dependences of the resonant field H_{res} of line one at $T=4$ K (a) and lines c (black dots) and d (white dots) at $T=292$ K (b) in Ge:Mn films ($x=4\%$). The solid lines are approximations by the Eq. (3), as described in the text. The inset shows orientations of rf and dc magnetic fields and the direction of the sample rotation. In our experimental set-up $\varphi=0$. At $\Theta_H=0$ the dc magnetic field lies in the film plane.

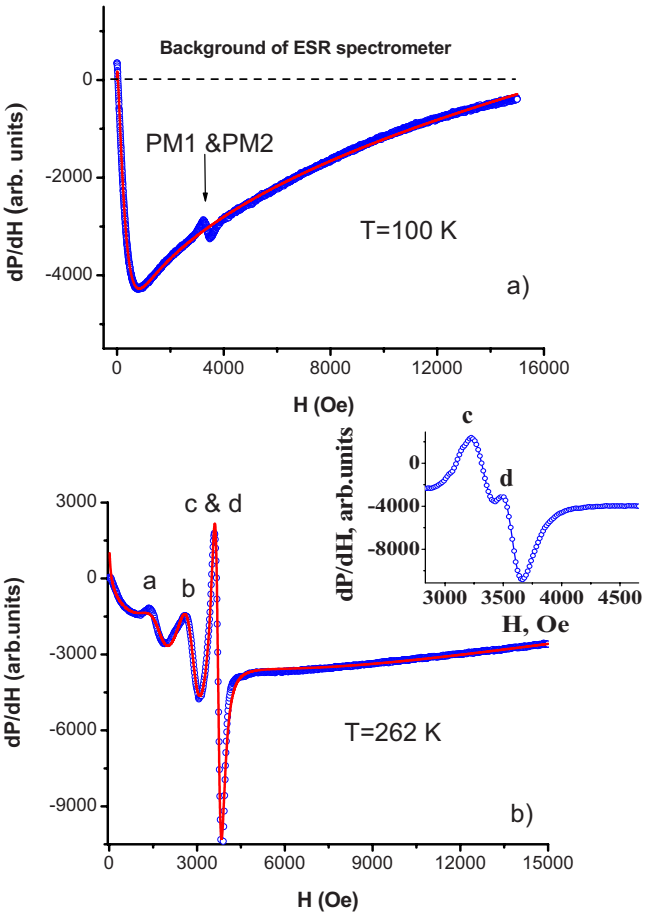

FIG. 5. (Color online) ESR spectra of the Ge:Mn film ($x=4\%$) at (a) $T=100$ K and (b) $T=262$ K. The dc magnetic field is parallel to the film plane. Details of ESR spectra (for lines c and d) are shown in the inset in Fig. 5(b). The dashed black line in Fig. 5(a) shows a background of the ESR spectrometer. The solid red line in Fig. 5(a) is an approximation to the magnetoresistance background using the Eq. (5), as described in the text. The solid red line in Fig. 5(b) is modeled by Lorentzian line fitting superimposed with a nonlinear magnetoresistance background.

spin excitations driven by the magnetic anisotropy of the whole layer, which in turn is the result of both magnetocrystalline and magnetoelastic components of the matrix anisotropy as well as the anisotropy of Mn_5Ge_3 clusters. The angular dependence of the resonant field of line one indicates the presence of a perpendicular component of the magnetization in zero field.[23] Similar results were observed for the lines two and three. A fit of the experimental results for angular dependencies of the resonant field given by the system of Eq. (3) is shown in Fig. 4(a) (solid line) at $T=4$ K. The figure shows good agreement between the experimental results and the model. The value $\theta=23°$, obtained by solving the system of Eq. (3), indicates that the magnetization vector is tilted away from the film plane and confirms the presence of the perpendicular magnetization component.

B. Intermediate-temperature regime ($T=60-220$ K)

Figure 5(a) shows an absorption spectrum dP/dH vs H at $T=100$ K. The spectrum differs significantly from that observed at low temperatures. It contains only the temperature-independent paramagnetic resonances PM1 and PM2. A strong nonlinear background, exceeding the background of the spectrometer with an empty holder by a few orders of magnitude, dominates the spectrum. In order to clarify the nature of this background, we investigated the resonant spectra at X-band ($f\cong 9.45$ GHz) and K-band ($f\cong 24.17$ GHz) frequencies. The paramagnetic resonances showed the expected frequency shift ($\cong 2.6$ times) to higher magnetic fields, whereas the large background signal remained frequency independent. This implies that this field- and temperature-dependent background, which was not observed in the undoped reference sample, might be caused by the microwave MR of the film.

C. High-temperature regime ($T=220-310$ K)

As the temperature increases ($T\geq 220$ K), new very intense resonant peaks a-d appear on the MR background in the field range $H=1-4$ kOe [Fig. 5(b)]. Lines c and d are positioned very close, see insert in Fig. 5(b). It should be noted that we assign different symbols to the high- and low-temperature resonant lines in order to emphasize the difference in their nature, as will be discussed below. Integral intensities of these peaks are larger than the intensity of the calibration sample by ~ 2 orders of magnitude (Fig. 6) and strongly exceed the intensities of the lines PM1 and PM2,

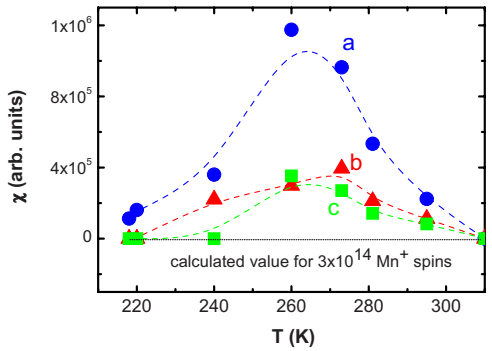

FIG. 6. (Color online) Temperature dependencies of the magnetic susceptibilities calculated for the lines *a*-*c* [see Fig. 5(b)] in the Ge:Mn film (x=4%). Dashed lines are guides for the eye.

which are completely masked by the lines *c* and *d*. The temperature dependence of the integral intensity, i.e., the magnetic susceptibility, of lines *a*, *b*, and *c* shows a maximum at T=260–270 K (Fig. 6) close to the Curie temperature Tc_3 (Ref. 34) measured by the SQUID magnetometer [Fig. 3(b)]. The lines *a*-*d* vanish at $T \geq 310$ K.

The out-of-plane angular dependence of the H_{res} values of lines *c* and *d* at 292 K is presented in Fig. 4(b). The dependence has a fourfold symmetry indicating that the magnetization vector $\boldsymbol{M}$ is oriented in the film plane.[23] The angular dependence of the line *b* (not shown) has a twofold character. This difference indicates that the line *b* and lines *c* and *d* have different microscopic origins, possibly related to ferromagnetic clusters with fourfold magnetocrystalline symmetry (lines *c* and *d*), a uniaxial anisotropy (line *b*) resulting from the shape anisotropy of a 2D film and a strongly inhomogeneous distribution of magnetic defects inside the film. Application of the system of Eq. (3) to the analysis of the angular dependence at T=250 K results in θ=0°, which indicates that the magnetization vector lies in the film plane with an experimental accuracy of ±10°. The magnetization curves recorded at T=250 K as a function of magnetic field (up to 5 T) also confirm that the easy axis of the magnetization is oriented in the plane of the film (Fig. 7). The magnetization does not saturate in high magnetic fields where its slope corresponds to the susceptibility $\Delta M/\Delta H$=6

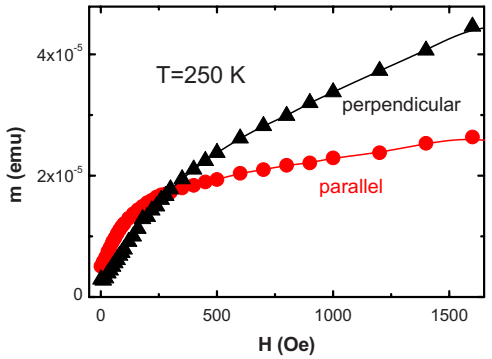

FIG. 7. (Color online) Field dependences of the magnetic moment m at T=250 K in the Ge:Mn thin film (x=8%) for parallel and perpendicular orientations of the dc magnetic field as indicated in the figure.

$\times 10^{-9}$ emu/Oe for the in-plane and $\Delta M/\Delta H$=18 $\times 10^{-9}$ emu/Oe for out-of-plane orientations. The observed $m(H)$ dependence is characteristic for a multicomponent magnetic system. Due to its magnitude and the strong angular dependence, this slope cannot be explained by paramagnetic impurities. Most likely, the shape of the curve can be attributed to the anisotropy of individual Mn_5Ge_3 precipitates and its interplay with the uniaxial anisotropy caused by a 2D nature of the thin Ge:Mn film.

It should be noted that the orientation dependence changes dramatically with temperature as evidenced by comparison with the line one at T=4 K in Fig. 4(a). The different angular dependences indicate that the magnetocrystalline anisotropy of the Ge:Mn film is temperature dependent and that the easy axis of the magnetization changes its direction with temperature.

IV. DISCUSSION

A. Transition temperatures

As the result of Mn implantation, the magnetic structure of the Ge:Mn film (x=4%) can be considered as consisting of two subsystems: (i) Ge_3Mn_5 nanoclusters with a mean size of 9.5 nm and separation of about 42 nm and (ii) individual Mn ions diluted in the germanium matrix.[32] These two systems have considerably different Curie temperatures: T_{C1} (diluted Mn ions) ≈15 K and $T_{C3}(Mn_5Ge_3)$=290–295 K, as reported in literature[35–37] and observed in our own experiments [Fig. 3(b)]. An additional transitional temperature, T_{C2}=60 K, was found in Mn-implanted Ge samples. Most probably, T_{C2} is the Curie temperature of some additional type of clusters, for example, a fraction of amorphous Ge:Mn precipitates, which become ferromagnetic below 60 K. A similar transition temperature was observed in MBE-grown Mn_5Ge_3 thin films and attributed to two magnetic sublattices with different exchange coupling constants and magnetocrystalline anisotropy.[38] Alternatively, T_{C2} might be related to the temperature at which a bound magnetic polaron (BMP) starts forming.[17,18,20,37] With decreasing temperature, such a quasiparticle consisting of localized charge carriers and Mn ions will expand and eventually percolate at T_{C1}. Thus, the whole Ge:Mn film becomes ferromagnetic below T_{C1}. Formation and merging of BMPs were previously observed in Ge:Mn films at ~76–112 K and ~12–16 K (Refs. 18 and 37). The existence of BMPs is generally consistent with transport properties of magnetic semiconductors. However, while T_{C1} in our experiments is in good agreement with other results, T_{C2} is somewhat lower. It should also be noted that usually the temperature corresponding to the formation of a BMP is not observed in direct experiment but rather obtained from the analysis of experimental data, i.e., reploting of the original $M(T)$ curve in $H/M(T)$ coordinates, approximating it with two linear dependencies and defining T_{C2} as an extrapolated divergence of the magnetic susceptibility.[20]

B. Electron spin resonance

As the distance between ferromagnetic Mn_5Ge_3 clusters is too large, no long-range magnetic order is possible at high

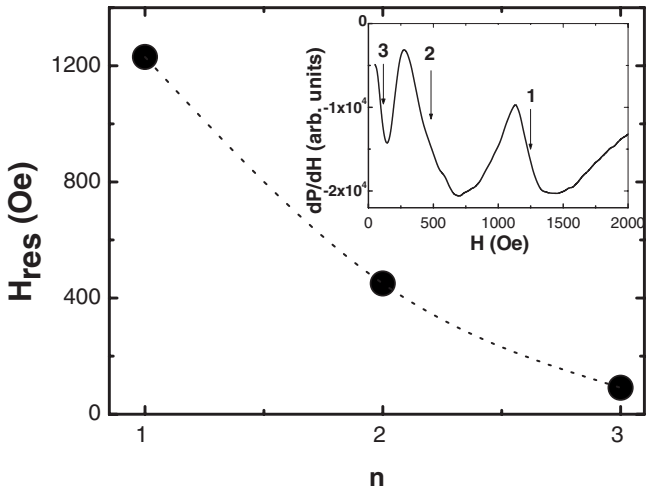

FIG. 8. Dependence of the resonant field H_{res} on the resonance peak number n in the Ge:Mn film ($x=4\%$) at $T=5$ K. The dashed line is an approximation by Eq. (4), as described in the text. The size of the symbols corresponds to the error bar. The insert shows positions of resonant fields at $T=5$ K. The dc magnetic field is normal to the film plane, $\theta_H=90°$.

temperatures ($T>220$ K). Therefore, the observed resonances [lines *a*-*d* in Fig. 5(b)] with different angular dependencies can be attributed to spin excitations in this and other types of ferromagnetic Ge:Mn clusters segregated in the Ge matrix.

Below T_{C1}, both clusters and diluted Mn ions form a long-range ordered magnetic state over the whole film. This is, for example, evidenced by the collective response of resonances 1–3, which show the same angular dependence at low temperature. In this state resonances from different clusters are exchange coupled yielding a similar response. Another possible origin of these low-temperature resonances is the excitation of standing spin-wave resonance.[39,40] Such spin waves can be excited both in perpendicular and parallel geometries[41,42] in ferromagnetic films with sufficient thickness. In the case of spin-wave resonances excited in the perpendicular orientation, one expects the following dependence of the resonant fields H_{res} on the spin-wave mode number n according to Ref. 42:

$$H_{res} = H_0 - \frac{D[3\pi/2(n+1/4)]^{2/3}}{t^2}, \tag{4}$$

where D is the bulk exchange stiffness constant and t is the film thickness.

We demonstrate that condition (4) for a spin-wave resonance is indeed fulfilled in our system for the lines 1–3 at low temperatures ($T=5$ K) assuming that the film thickness is $t=120$ nm, as shown in Fig. 8, and deduce the exchange stiffness constant $D=(0.85-1.15)\times 10^{-6}$ Oe cm^2. Depending on the rotation angle Θ_H, the exponent value varies from 0.4–0.7. Such deviations from 2/3 can be qualitatively explained by considering the longitudinal inhomogeneous structure of the film and temperature dependent change of the magnetic anisotropy. It should be noted that Eq. (4) is not fulfilled in one-dimensional (1D) $Ge_{1-x}Mn_x$ nanostructures of a similar chemical composition.[43] Thus, the spin-wave resonance has never been observed in $Ge_{1-x}Mn_x$ nanowires, which was also confirmed by different temperature dependences of resonant lines there.[10–12]

Observation of spin-wave resonances in our films indicates long-range magnetic ordering at low temperatures. It should be noted that it was impossible to detect this type of resonances in strongly spatially separated small Mn_5Ge_3 clusters at high temperatures. Thus, in addition to conventional ferromagnetism related to the Mn_5Ge_3 system, we observe long-range exchange interactions related to the ferromagnetic nature of diluted Mn ions dispersed in the nonmagnetic matrix.

C. Magnetoresistance

The high-frequency MR can be measured in doped semiconductors by means of ESR spectroscopy as was discussed in the introduction [see Eq. (1)]. Our experimental results show that in low magnetic fields the derivative of the microwave absorption, dP/dH, is negative (Fig. 5). The best approximation to this sharply decreasing part of the MR signal is given by $dP/dH=A[1-\exp(BH^q)]$, where A and B are field-independent coefficients. The derivative passes a temperature-dependent minimum at $H\cong 1-4$ kOe (Fig. 5). The high-field part of the MR was approximated by the function $dP/dH=CH^p$, where C is the constant. Numerical values of A and C depend on a number of factors, such as the sample geometry and size. On the other hand, exponents p and q reflect the physical nature of the MR. Below we analyze the temperature and angular dependences of these parameters only. A good fit to the experimental background [Fig. 5(a)] is obtained using,[44]

$$dP/dH = A[1-\exp(BH^q)] + CH^p. \tag{5}$$

The angular dependencies of the exponents $q(\Theta)$ and $p(\Theta)$ are shown in Fig. 9. First, we discus the low-field part of the MR. When the sample rotates around the axis lying in its plane [see inset in Fig. 4(a)], the q value varies in the range 0.99–1.20 [Fig. 9(a)]: for $\Theta=90°$ (dc magnetic field is normal to the sample plane) we obtain $q\cong 1.0$. This indicates that the MR occurs due to Zeeman splitting of charge-carrier states,[45] which are degenerate in zero magnetic fields. The applied magnetic field lifts the degeneracy and leads to splitting of the states. As the result, the probability of hopping, carrier mobility, and density of states will be changed. In the frame of this model one calculates the coefficient $B=-(2-4)\times 10^{-4}$ G$^{-1}\approx \mu_0\mu_B gS(S+1)/kT$ (where k is the Boltzmann constant, μ_B is the Bohr magneton, T is the temperature, and $S=1/2$), which is in good agreement with the value $B=4\times 10^{-4}$ G^{-1} obtained from the fit in Fig. 5(b) at $T=262$ K. When the external magnetic field is tilted away from the sample normal, an additional component of the MR appears. In particular, for $\Theta=0°$ (dc magnetic field is in the sample plane) we find $q=1.2$, which indicates a rather significant deviation from the simple Zeeman model described above. This can be explained by the additional contribution of the anisotropic MR that is superimposed on the hopping Zeeman MR, which is usually isotropic. The anisotropy of

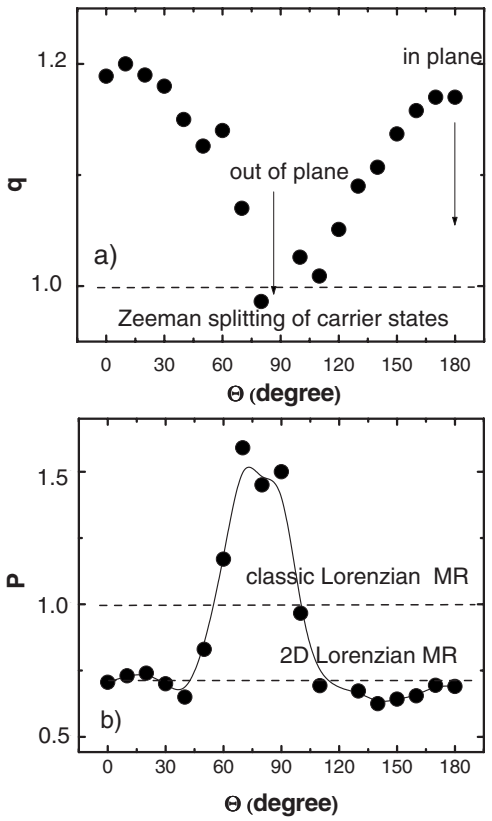

FIG. 9. Angular dependencies of q (upper panel) and p (lower panel) exponents [Eq. (5)] at $T=270$ K describing low- and high-field components of the magnetoresistance, respectively. The size of the symbols corresponds to the error bar. Horizontal lines show predictions corresponding to different magnetoresistance models. The solid line in (b) is a guide for the eye.

the low-field part of the MR found in our experiments may cause limitation of wave functions in two-dimensional films as it was found in Refs. 46 and 47. Another possible reason of the MR anisotropy is an inhomogeneity of the demagnetization field due to an uneven distribution of various magnetic centers in the Ge:Mn film.

The parameter p characterizing the quasilinear high-field part of the MR varies in the range 0.70–1.55 [Fig. 9(b)], in particular, $p=0.70\pm0.06$ when $\Theta=0°$ and $p=1.55\pm0.05$ when $\Theta=90°$. These values of p are compatible with the Lorentzian MR existing in most conductors and semiconductors as a result of orbital motion of charge carriers in the magnetic field. Deviation of p from one is typical for conductive systems with reduced dimensions and a high dopant concentration.[48,49] In particular, a relatively low value of $p=0.5-0.8$ is expected for two-dimensional disordered semiconductors with high dopant level (as in our case).[48] The effect is caused by heavy doping and strong disorder of the crystal lattice that leads to a spin-dependent scattering of charge carriers. The theoretical background for this case has been given in Ref. 48. The orientation dependences of q and p exponents are likely to be related to the magnetocrystalline anisotropy of Mn_5Ge_3 clusters acting as scattering centers for charge carriers. Another possible reason of the anisotropy is a quasi-one-dimensional character of the disorder, for example, due to formation of conductive channels caused by Mn implantation.

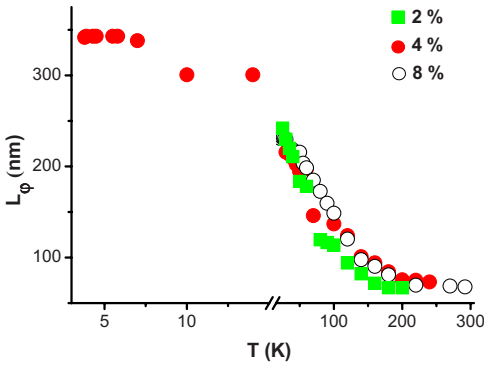

FIG. 10. (Color online) Temperature dependencies of the phase relaxation length of the carriers in the Ge:Mn films doped with 2%, 4%, and 8% of Mn. The size of the symbols corresponds to the error bar.

It is important to note, that the field-dependent MR has not been observed in one-dimensional DMS nanostructures of a similar chemical composition [$Ge_{1-x}Mn_x$ nanowires ($x=1-5\%$), see Refs. 10–12]. Thus, one may conclude that reducing the dimension from 2D to quasi-one-dimensional suppresses the spin-dependent scattering in the Ge:Mn system.

D. Phase relaxation length of carriers

Veinger *et al.*[27] have shown that the field-dependent MR has a minimum at some characteristic magnetic field, $H_{\varphi,}$, where the phase coherence of the charge carriers is destroyed. This field is related to the carrier dephasing length, L_φ, as

$$H_\varphi = \frac{\hbar c}{4eL_\varphi^2}, \tag{6}$$

where all other symbols are conventional. We have adopted the same procedure and calculated L_φ for all investigated samples (Fig. 10). For the film with $x=4\%$, $L_\varphi(T)$ saturates at low temperatures, $T\leq 15$ K, where the phase relaxation length reaches its maximal value, $L_\varphi\cong 350$ nm. Thus, the phase relaxation length is much smaller than the skin-depth over the whole temperature range. On the other hand, L_φ exceeds the thickness ($t=120$ nm) at $T=4-100$ K. This implies the existence of three-dimensional conductivity in the semiconductor films. At high temperatures ($T>150$ K) the phase relaxation length is reduced to $L_\varphi\cong 70$ nm, i.e., within the thickness of the magnetically modified layer. This value is still notably higher than the mean distance between Mn_5Ge_3 clusters, which is about 42 nm for $x=4\%$. This fact suggests that the Mn_5Ge_3 clusters do not noticeably hinder the carrier mobility even at high temperatures. Moreover, since the phase relaxation length significantly exceeds the cluster size, the intrinsic conductivity of the nanoclusters does not generally influence the MR, i.e., all observed features of the MR are mainly "cluster-independent" and related to the Ge matrix with diluted Mn ions. Thus, we conclude

that the main contribution to the microwave MR originates from charge carriers.

V. CONCLUSIONS

The microwave absorption in Mn-implanted Ge thin films with dopant concentrations of 2%, 4%, and 8% has been investigated. At high temperatures ($T=220-290$ K) resonant peaks correspond to the ESR in ferromagnetic Mn_5Ge_3 clusters. On the other hand, low-temperature resonances ($T=4-60$ K) can be interpreted as arising from spin-wave excitations and obeying the expected dispersion law [see Eq. (4)]. The appearance of spin-wave resonances at low temperatures indicates the presence of long-range spin states and the cooperative magnetic response originating from spin ordering in the whole system.

We show that the magnetoresistive background contains two components: a positive classic Lorentzian magnetoresistance and a negative one arising from the Zeeman splitting. The orientation dependences of both components are explained by a superposition of the isotropic part of the MR due to Zeeman splitting of the charge-carriers states and its anisotropic part caused by dimensional limitations in the thin film. The analysis of the magnetoresistance background enables to calculate the phase relaxation length of charge carriers that varies in the range 70–350 nm as the temperature decreases from 300 to 4 K. Since this length exceeds significantly the cluster size, all observed features of the magnetoresistance are cluster-independent and can be attributed to charge carriers in the Ge matrix. Comparison of the magnetoresistance in Ge:Mn thin films and nanowires indicates dimensional limitations on the effect of spin-dependent scattering in the Ge:Mn system. We demonstrate a very good correlation between the ESR and SQUID magnetometry results. These techniques allow us to elucidate a complex magnetic structure of the Ge:Mn films and distinguish contributions from several types of magnetically ordered clusters and diluted ions.

ACKNOWLEDGMENTS

This work was partially funded under the UK DIUS's NMS under Project No. ESQ01T1 and by the Deutsche Forschungsgemeinschaft, Sonderforschungsbereich Grant No. 491.

*olga.kazakova@npl.co.uk

[1] T. Dietl, Nat. Mater. **2**, 646 (2003).
[2] T. Dietl, J. Phys.: Condens. Matter **19**, 165204 (2007).
[3] J. S. Kulkarni, O. Kazakova, D. Erts, M. Morris, M. T. Shaw, and J. D. Holmes, Chem. Mater. **17**, 3615 (2005).
[4] O. Kazakova, J. S. Kulkarni, J. D. Holmes, and S. O. Demokritov, Phys. Rev. B **72**, 094415 (2005).
[5] J. S. Kulkarni, O. Kazakova, and J. D. Holmes, Appl. Phys. A: Mater. Sci. Process. **85**, 277 (2006).
[6] M. Jamet, A. Barski, T. Devillers, V. Poydenot, R. Dujardin, P. Bayle-Guillemaud, J. Rothman, E. Bellet-Amalric, A. Marty, J. Cibert, R. Mattana, and S. Tatarenko, Nat. Mater. **5**, 653 (2006).
[7] H. W. Wu, C. J. Tsai, and L. J. Chen, Appl. Phys. Lett. **90**, 043121 (2007).
[8] O. Kazakova, J. S. Kulkarni, D. C. Arnold, and J. D. Holmes, J. Appl. Phys. **101**, 09H108 (2007).
[9] T. Devillers, M. Jamet, A. Barski, V. Poydenot, P. Bayle-Guillemaud, E. Bellet-Amalric, S. Cherifi, and J. Cibert, Phys. Rev. B **76**, 205306 (2007).
[10] R. B. Morgunov, A. I. Dmitriev, I. B. Klenina, J. S. Kulkarni, J. D. Holmes, and O. L. Kazakova, J. Magn. Magn. Mater. **316**, 210 (2007).
[11] R. B. Morgunov, A. I. Dmitriev, Y. Tanimoto, I. B. Klenina, O. L. Kazakova, J. S. Kulkarni, and J. D. Holmes, Phys. Solid State **49**, 296 (2007).
[12] R. B. Morgunov, Y. Tanimoto, I. B. Klenina, J. S. Kulkarni, J. D. Holmes, and O. L. Kazakova, J. Magn. Magn. Mater. **310**, e824 (2007).
[13] S. Cho, S. Choi, S. C. Hong, Y. Kim, J. B. Ketterson, Bong-Jun Kim, Y. C. Kim, and Jung-Hyun Jung, Phys. Rev. B **66**, 033303 (2002).
[14] Y. D. Park, A. Wilson, A. T. Hanbicki, J. E. Mattson, T. Ambrose, G. Spanos, and B. T. Jonker, Appl. Phys. Lett. **78**, 2739 (2001).
[15] Y. D. Park, A. T. Hanbicki, S. C. Erwin, C. S. Hellberg, J. M. Sullivan, J. E. Mattson, T. F. Ambrose, A. Wilson, G. Spanos, and B. T. Jonker, Science **295**, 651 (2002).
[16] F. Tsui, L. He, L. Ma, A. Tkachuk, Y. S. Chu, K. Nakajima, and T. Chikyow, Phys. Rev. Lett. **91**, 177203 (2003).
[17] N. Pinto, L. Morresi, M. Ficcadenti, R. Murri, F. D'Orazio, F. Lucari, L. Boarino, and G. Amato, Phys. Rev. B **72**, 165203 (2005).
[18] A. P. Li, J. Shen, J. R. Thompson, and H. H. Weitering, Appl. Phys. Lett. **86**, 152507 (2005).
[19] Sang Soo Yu, Tran Thi Lan Anh, Young Eon Ihm, Dojin Kim, Hyojin Kim, Soon Ku Hong, Sangjun Oh, Chang Soo Kim, Hwack Joo Lee, and Byung Chill Woo, Curr. Appl. Phys. **6**, 545 (2006).
[20] A. P. Li, J. F. Wendelken, J. Shen, L. C. Feldman, J. R. Thompson, and H. H. Weitering, Phys. Rev. B **72**, 195205 (2005).
[21] H. Li, Y. Wu, Z. Guo, P. Luo, and S. Wang, J. Appl. Phys. **100**, 103908 (2006).
[22] S. H. Song, S. H. Lim, M. H. Jung, T. S. Santos, and J. S. Moodera, J. Korean Phys. Soc. **49**, 2386 (2006).
[23] M. Farle, Rep. Prog. Phys. **61**, 755 (1998).
[24] X. Liu and J. K. Furdyna, J. Phys.: Condens. Matter **18**, R245 (2006).
[25] C. Antoniak, J. Lindner, V. Salguerino-Maceira, and M. Farle, Phys. Status Solidi A **203**, 2968 (2006).
[26] R. Skomski, J. Phys.: Condens. Matter **15**, R841 (2003).
[27] A. I. Veinger, A. G. Zabrodskii, and T. V. Tisnek, Semiconductors **34**, 746 (2000).
[28] A. I. Veinger, A. G. Zabrodskii, and T. V. Tisnek, Phys. Status Solidi B **230**, 107 (2002).

[29] L. Ottaviano, M. Passacantando, S. Picozzi, A. Continenza, R. Gunnella, A. Verna, G. Bihlmayer, G. Impellizzeri, and F. Priolo, Appl. Phys. Lett. **88**, 061907 (2006).
[30] M. Passacantando, L. Ottaviano, F. D'Orazio, F. Lucari, M. DeBiase, G. Impellizzeri, and F. Priolo, Phys. Rev. B **73**, 195207 (2006).
[31] L. Ottaviano, P. Parisse, M. Passacantando, S. Picozzi, A. Verna, G. Impellizzeri, and F. Priolo, Surf. Sci. **600**, 4723 (2006).
[32] L. Ottaviano, M. Passacantando, A. Verna, R. Gunnella, E. Principi, A. Di Cicco, G. Impellizzeri, and F. Priolo, J. Appl. Phys. **100**, 063528 (2006).
[33] R. M. White, *Quantum Theory of Magnetism, Magnetic Properties of Materials*, 3rd ed. (Springer, New York, 2006), p. 366.
[34] M. Farle and K. Baberschke, Phys. Rev. Lett. **58**, 511 (1987).
[35] N. Yamada, J. Phys. Soc. Jpn. **59**, 273 (1990).
[36] C. Jaeger, C. Bihler, T. Vallaitis, S. T. B. Goennenwein, M. Opel, R. Gross, and M. S. Brandt, Phys. Rev. B **74**, 045330 (2006).
[37] C. Bihler, C. Jaeger, T. Vallaitis, M. Gjukic, M. S. Brandt, E. Pippel, J. Woltersdorf, and U. Gösele, Appl. Phys. Lett. **88**, 112506 (2006).
[38] C. Zeng, S. C. Erwin, L. C. Feldman, A. P. Li, R. Jin, J. R. Thompson, and H. H. Weitering, Appl. Phys. Lett. **83**, 5002 (2003).
[39] C. Kittel, Phys. Rev. **110**, 1295 (1958).
[40] M. H. Seavey and P. E. Tannenwald, Phys. Rev. Lett. **1**, 168 (1958).
[41] N. M. Salanskij and M. Sh. Erukhimov, *Physical Properties and Applications of Magnetic Films* (Nauka, Moscow, 1975).
[42] B. Hoekstra, R. P. Stapele, and J. M. Robertson, J. Appl. Phys. **48**, 382 (1977).
[43] See EPAPS Document No. E-PRBMDO-77-114824 for dependence of the resonant field B_{res} on the mode number $n^{2/3}$ in the Ge:Mn thin films and nanowires at $T=5$ K. For more information on EPAPS, see http://www.aip.org/pubservs/epaps.html
[44] R. P. Khosla and J. R. Fisher, Phys. Rev. B **2**, 4084 (1970).
[45] I. Kubelik and A. Triska, J. Phys. B **23**, 115 (1973).
[46] V. Yu. Butko, J. F. DiTusa, and P. W. Adams, Phys. Rev. Lett. **85**, 162 (2000).
[47] B. I. Shklovskii and B. Z. Spivak, in *Hopping Transport in Solids*, edited by M. Pollak and B. Shklovskii (Elsevier, Amsterdam, 1991), p. 271.
[48] M. M. Parish and P. B. Littlewood, Nature (London) **426**, 162 (2003).
[49] H. Roth, W. D. Straub, W. Bernard, and J. E. Mulhern, Phys. Rev. Lett. **11**, 328 (1963).